Journal of Thermal Analysis and Calorimetry (2018) 132:919–926
https://doi.org/10.1007/s10973-018-7026-0

Synergistic flame-retardant effects of aluminum phosphate and Trimer in ethylene–vinyl acetate composites

Guang Yang[1] · Weihong Wu[2] · Huanxin Dong[1] · Yonghui Wang[1] · Hongqiang Qu[1] · Jianzhong Xu[1]

Received: 30 June 2017 / Accepted: 18 January 2018 / Published online: 25 January 2018

Abstract
A series of flame-retardant ethylene–vinyl acetate (EVA) composites with different contents of aluminum phosphate (AHP) and Trimer were prepared. The synergistic flame-retardant effects of the Trimer with AHP in EVA/AHP blends were studied by limiting oxygen index (LOI) tests, UL-94 tests, cone calorimeter tests, thermogravimetric analysis, and scanning electron microscopy (SEM). The LOI and UL-94 results showed that the system containing AHP and Trimer was very effective in improving the flame retardancy of EVA. When the mass ratio of AHP and Trimer was 3:1, the highest flame retardancy could be obtained, and when the flame-retardant loading was 30 wt%, the EVA/AHP/Trimer (7.5%) sample could achieve the V-0 rating in UL-94 tests, at the same time, its LOI value was 24.4%. The TG and DTG results showed that the addition of flame retardants catalyzes EVA decomposition in the first stage and generates a more stable char residue in the second stage. Consequently, an efficient reduction in the flammability parameters, such as heat release rate, total heat release, smoke production rate, and total smoke production could be observed. In addition, it was observed from the SEM observations of the morphological features that the AHP and Trimer combination, at the optimum proportion, could promote the formation of compact charred layers and prevent their cracking, which effectively protected the underlying materials from burning.

Keywords Aluminum phosphate · Trimer · Flame retardant · Smoke suppression · EVA

Introduction

Ethylene–vinyl acetate copolymer (EVA) resins are copolymers of ethylene and vinyl acetate monomers. Unlike in pristine polyethylene, a vinyl acetate monomer is introduced along with an ethylene monomer into the molecular chain of EVA, leading to a reduction in the degree of crystallinity, improvement in flexibility, increase in impact resistance, increase in the heat sealing property, and improvement in compatibility with fillers. Therefore, EVA has a potentially wide range of applications in various fields such as electronic devices, electrical engineering, wires and cables, buildings and transportation (air crafts, cars) [1, 2]. However, EVA is flammable and undergoes serious melting during its combustion, which limits its further applications [2].

It is well known that inorganic hydroxide fire retardants such as $Mg(OH)_2$ and $Al(OH)_3$ are environmentally friendly and can be used with EVA polymeric materials. However, as the flame-retardant efficiency of these materials is low, large amount of these materials are required to achieve a high flame-retardant effect. This inevitably deteriorates the mechanical properties and processing performance of the polymeric material. By controlling the particle size and morphology, surface performance, and dispersion properties of these inorganic hydroxides in the matrix resin, the flame retardancy of the EVA resins can be improved [3, 4]. Moreover, the usage of synergistic materials, such as fumed silica [5], sepiolite [6], nanoclay [7], cerium oxide [8], and ammonium polyphosphate [9], can

Jianzhong Xu's contribution to the article is equivalent to the correspondence author.

✉ Hongqiang Qu
hqqu@163.com

[1] Key Laboratory of Analytical Science and Technology of Hebei Province, College of Chemistry and Environmental Science, Hebei University, Baoding 071002, Hebei, People's Republic of China

[2] College of Science, Agriculture University of Hebei, Baoding 071000, Hebei, People's Republic of China

effectively improve the flame-retardant efficiency of these inorganic hydroxides.

Intumescent flame retardants and some novel phosphorous compounds are two other types of flame-retardant additives that are often used with EVA [10–13]. Wang et al. synthesized a phosphorus-containing flame retardant, 4-(5,5-dimethyl-2-oxo-1,3,2-dioxaphosphorinan-2-yloxy-methyl)-2,6,7-trioxa-1-phosphabicyclo[2.2.2]octane-1-oxide (MOPO), and investigated the flame retardancy and thermal behavior of MOPO and ammonium polyphosphate (APP) in EVA. The results showed that the heat release rate (HRR) and total heat release (THR) of EVA composites were decreased significantly and rich compact char layers were generated in the condensed phase [10]. Alongi et al. [11] synthesized cyclodextrin nanosponges containing phosphorus compounds to enhance the combustion properties of EVA. Wang et al. synthesized a novel organic–inorganic hybrid flame retardant consisting of a brucite core and dodecylamine polyphosphate shell: According to the cone, UL-94, and limiting oxygen index (LOI) test results, this novel organic–inorganic hybrid compound had excellent flame-retardant properties. This remarkable effect was obtained by nanoengineering the core/shell-structured brucite@polyphosphate@amine hybrid system, which facilitated the formation of an intact and compact residue with a fence structure during the burning process [12]. Liu et al. used a Schiff-base polyphosphate ester (PAB) and organophilic montmorillonite (OMMT) as flame retardants for EVA, and their synergistic flame-retardant effect was investigated. The results revealed that OMMT platelets selectively dispersed in the PAB phase reacted with the phosphoric acid generated from PAB and formed a silicoaluminophosphate (SAPO) structure [13]. These organic phosphorous compounds have proved considerably efficient as flame retardants in EVA, but their manufacture on an industrial scale is relatively complex and expensive, which limits their usage. Therefore, inorganic phosphorus-based flame retardants (such as hypophosphites [14] and pyrophosphates [15]), which have a flame-retardant mechanism similar to that of organic phosphorus compounds, have become the subject of research. Metal hypophosphite compounds, such as aluminum hypophosphite (AHP), magnesium hypophosphite, and cerium hypophosphite, have attracted much attention over the past few decades for their high thermal and chemical stability, good mechanical and electrical properties, and environmental-friendly characteristics [16–18]. In particular, AHP is expected to replace halogen-based flame retardants. Thus far, it has been applied to enhance the flame-retardant properties of different polymers, such as glass-filled polyamide 6 [17], polybutylene terephthalate (PBT) [19], and polylactide [20].

In the present, AHP and tri(1-oxo-2,6,7-trioxa-1-phosphabicyclo [2] octane-methyl)-phosphate (Trimer) were chosen to develop environmental-friendly EVA composites with enhanced flame retardancy. Owing to its high phosphorus content (21%), Trimer has excellent thermal stability and induces a good charring effect [21]. The synergistic smoke suppression properties and flame-retardant effects obtained using AHP and Trimer were investigated by LOI testing, cone calorimeter testing (CCT), and thermogravimetric analysis (TG).

Experimental

Materials

EVA (14-2) was purchased from Beijing Eastern Petrochemical Co., Ltd. Organic Chemical Plant, China. The basic properties of EVA are as follows: vinyl acetate (VA) content of 14%, density 0.935 g cm^{-3}, hardness 92A (ISO868), vicat softening point 70 °C, and elongation at break 720%. AHP was provided by Wuhan Hanye Chemical New Material Co., Ltd., China. Trimer was supplied by Jiang su Yoke Technology Co., Ltd., China. The structure of Trimer is illustrated in Scheme 1.

Sample preparation

EVA and all additives were dried at 80 °C over night before use. A certain amount of EVA was melted in the mixer at 135 °C. Then, a certain amount of AHP and Trimer were added into the mixer, respectively. The blends were mixed for 10 min and pressed into sheets using tablet press machine. The formulations of flame-retardant EVA composites are listed in Table 1.

Limiting oxygen index (LOI)

The LOI values were determined in accordance with ASTM standard D2863-2000 using a JF-3 oxygen index meter (Jiangning Analytical Instrument Factory, China). The specimens used for the test were of dimensions

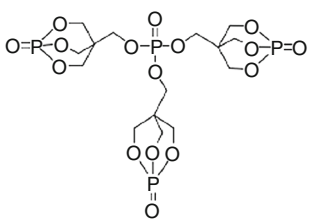

Scheme1 Structure of Trimer

Table 1 Combustibility of flame-retardant EVA

Sample	Formulation/ %			LOI/%	UL-94/3.2/mm		
	EVA	AHP	Trimer		Dripping	t_1/t_2^a	Rating
1	100	0	0	19.0	Yes	BC[b]	No rating
2	70	30	0	24.0	No	BC	No rating
3	65	35	0	24.5	No	0.4/5.0	V-0
4	60	40	0	25.0	No	0.4/1.4	V-0
5	70	0	30	23.5	Yes	11.5/7.5	V-2
6	70	24	6	24.6	No	8.6/14.2	V-1
7	70	22.5	7.5	24.4	No	0.3/1.0	V-0
8	70	20	10	24.2	No	0.5/14.6	V-1
9	70	15	15	23.9	Yes	BC	No rating
10	70	10	20	23.2	Yes	BC	No rating
11	70	7.5	22.5	23.5	No	0.6/1.2	V-0

[a] Description of combustion phenomena and results in the ul-94 test process.

[b] t_1/t_2, the average time of the first and second burning times for five specimens in UL-94 test. BC, burning to the clamp

$10 \times 6.5 \times 3$ mm^3. Each sample was tested for 5 times. And, the LOI value was the average of the 5 values.

The UL-94 test

The UL-94 test was carried out using a CZF-3 vertical flammability tester (Jiangning Analytical Instrument Factory, China) according to ASTM standard D3801-2006. Five specimens of each sample were tested in UL-94 vertical burning test.

Cone calorimeter

Cone calorimetry was performed using a cone calorimeter (Fire Testing Technology Ltd., UK) according to ISO Standard 5660. Each specimen ($100 \times 100 \times 3$ mm^3) was wrapped in aluminum foil and exposed horizontally to a 50 kW m^{-2} external heat flux.

Three samples were carried out on the cone calorimeter test. The corresponding values of different parameters are average values of the three tests in this paper.

Scanning electron microscopy

The morphology of the char residues was measured by scanning electron microscopy (SEM, JSM-7500, JEOL) with the acceleration voltage of 15 kV.

Thermogravimetric analysis

Thermogravimetric analysis (TG) and derivative thermogravimetric analysis (DTG) were performed using a STA 449C thermal analyzer (Netzsch, Germany). About 10.0 mg of sample was put in an alumina crucible and heated from ambient temperature to 800 °C. The heating rates were set as 10 °C min^{-1} (nitrogen atmosphere, flow rate of 60 mL min^{-1}).

Results and discussion

Flame-retardant properties

Composite fillers with different proportions of AHP and Trimer were prepared and used as flame-retardant fillers in EVA. LOI and UL-94 tests were performed to investigate the flame retardancy of each formulation; the results are summarized in Table 1. It is found that pure EVA combusts easily (LOI value of 19.0%) and is not classified in the UL-94 rating. In the UL-94 test, it can be observed that severe combustion is followed by rapid diffusion of the flame and intense dripping from EVA samples, owing to the highly combustible nature of EVA. The LOI value of EVA gradually increased with an increase in the amount of the added AHP. The LOI values increased from 19.0 to 24.0 and 25.0% when the AHP loadings were 30 and 40 mass%, respectively. In the UL-94 test, when the AHP content was less than 30 mass%, although the dripping phenomenon is obviously suppressed, the 3.2-mm EVA sample was not eligible for the V-0 rating. As the AHP level increased to 35 mass%, the combustion behavior of the EVA composite was further influenced and a V-0 rating could be achieved. When 30 mass% Trimer was added to the composite, the LOI value of EVA sample increased to 23.5%, and a V-2 rating in the UL-94 standard was achieved. These results indicate that AHP or Trimer alone cannot effectively improve the flame retardancy of EVA. When AHP and Trimer were added together to the EVA

matrix at a mass ratio of 3:1 or 2:1, the observed LOI values were slightly higher than that of EVA containing AHP alone. Furthermore, the samples displayed a UL-94 V-0 rating when the mass ratio of AHP and Trimer was either 3:1 or 1:3. This suggests that this novel combination of flame retardants can enhance the drip resistant of EVA.

Cone calorimetry

The cone calorimeter is an effective bench-scale apparatus to evaluate the forced combustion behavior of polymeric materials [22, 23]. The flame retardancy of AHP, Trimer, and AHP/Trimer (mass ratio, 3:1 and 1:2)-loaded EVA matrices (30 mass% loading) was quantified by cone calorimetry at radiation of 50 kW m^{-2}. The results are summarized in Figs. 1–4 and Table 2.

As shown in Fig. 1, the HRR curve for neat EVA exhibited a sharp peak, which can be explained by the combustion behavior of the sample. At a heat flux of 50 kW m^{-2}, the surface of neat EVA melts and a thin layer of char is formed. The charred surface remains intact for a short period leading to a small peak in the HRR curve. Subsequently, the charred surface is destroyed by vigorous gas expulsion from the underlying sample. As more

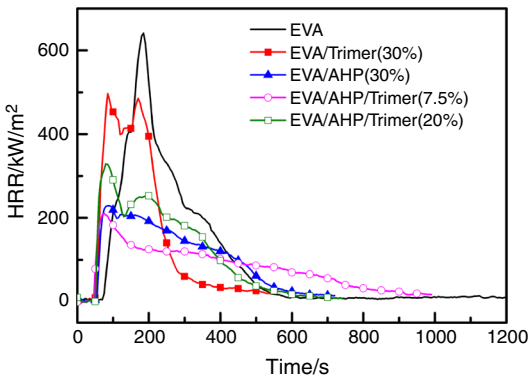

Fig. 1 HRR of samples under heat flux 50 kW m^{-2}

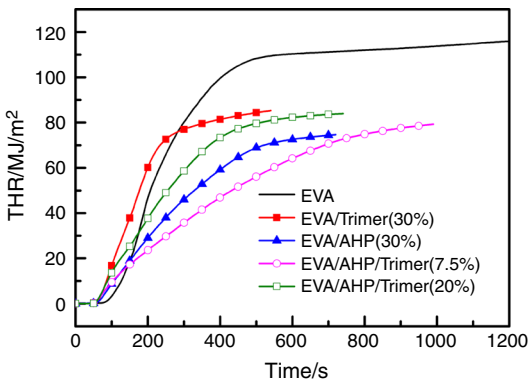

Fig. 2 THR of samples under heat flux 50 kW m^{-2}

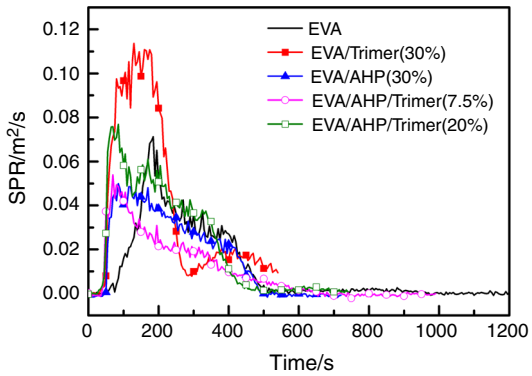

Fig. 3 SPR of samples under heat flux 50 kW m^{-2}

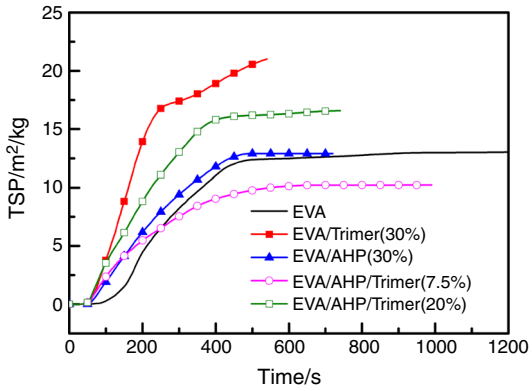

Fig. 4 TSP of samples under heat flux 50 kW m^{-2}

flammable gases were released into the environment, the specimen burned more intensely, reaching a peak HRR (PHRR) of 639.59 kW m^{-2} after 180 s of irradiation. As the sample has been burning consumption, the HRR value reduced gradually. After approximately 700 s, the HRR value is close to zero, as shown in the HRR curve, indicating that the basic burning of neat EVA was completed.

As compared to neat EVA, the HRR curve of the EVA/Trimer (30%) composite exhibited a bimodal behavior. The two PHRR values of the EVA/Trimer (30%) composite are 494.62 and 485.42 kW m^{-2}, which are lower than the PHRR value of the neat EVA sample. Meanwhile, the time to ignition (TTI) decreased and the first HRR peak of the EVA/Trimer (30%) sample occurred significantly earlier than the HRR peak of neat EVA. These results suggest that Trimer facilitates the formation of char on the EVA/Trimer (30%) composite surface and maintain the integrity of the char layer formed during the early stages of combustion. As the protective layer is broken, allowing further combustion, another obvious peak appeared in the HRR curve.

AHP can promote the formation of char on polymers during combustion [14]. As compared to EVA/Trimer (30%), the EVA/AHP (30%) sample exhibited a lower PHRR of 229.76 kW m^{-2}, while the peak width increased.

Table 2 Cone calorimeter test results of EVA composite samples at a heat flux of 50 kW m^{-2}

	EVA	EVA/AHP (30%)	EVA/Trimer (30%)	EVA/AHP/Trimer (3:1)	EVA/AHP/Trimer (1:2)
PHRR/kW m^{-2}	639.59	229.76	494.62	210.73	329.85
$t_{PHRR/S}$	180	83	83	70	84
Av-HRR/kW m^{-2}	102.75	111.97	173.60	83.86	121.55
THR/MJ m^{-2}	116.33	74.95	85.53	79.06	84.17
Av-MLR/g s^{-1}	0.02	0.03	0.05	0.02	0.03
Av-EHC/MJ kg^{-1}	41.94	35.58	76.89	35.14	32.49
Av-SEA/m^2 kg^{-1}	531.30	687.06	829.34	501.40	720.17
PSPR/m^2 kg^{-1}	0.071	0.047	0.114	0.052	0.076
TSP/m^2 kg^{-1}	13.04	12.97	21.11	10.29	16.54
Av-COY/kg kg^{-1}	0.05	0.17	0.14	0.18	0.14
Av-CO_2Y/kg kg^{-1}	3.30	2.59	2.08	2.87	2.45

These results indicate that AHP can increase the speed of firm char formation, thus protecting the underlying material. Therefore, the decrease in HRR occurs sooner. When AHP and Trimer in optimum proportions were present together in the composite, the HRR of the sample was further reduced during combustion; the PHRR of EVA/AHP/Trimer (7.5%) decreased by 67% as compared to neat EVA. This suggests the formation of a more stable char residue during the combustion process. This could explain why the UL-94 rating of EVA/AHP/Trimer (7.5%) is higher than that of EVA/AHP (30%).

Corresponding to the HRR curve, the THR curves of the EVA samples are shown in Fig. 2. As shown in the figure, the THR value for neat EVA increases linearly with increasing irradiation time and becomes constant after 500 s. An obvious reduction can be observed between the THR values of the neat sample and the flame-retardant samples. The EVA/AHP/Trimer (7.5%) sample has a minimum THR value before 710 s, after which its THR value continues to increase upon irradiation; despite this increasing trend, the final THR value is obviously not as good as in the previous stage. These results might be attributed to the slow glowing combustion of the residual char, owing to which the THR value gradually increased until the end of the test [24].

In contrast to the HRR curve, the SPR of neat EVA had a low value after the burning started. Therefore, the TSP, peak SPR (PSPR), and average specific extinction area (Av-SEA) of neat EVA are smaller than those of the EVA/Trimer (30%) and EVA/AHP/Trimer (20%). This is mainly because of the molecular structure of EVA and its degradation pathway [25].

As compared to neat EVA, the SPR curve of the EVA/Trimer (30%) composite shows a bimodal phenomenon, and after the material being ignited, the SPR rose sharply to a high level between 75 and 230 s. This corresponds to the highest SPR, Av-SEA, PSPR, and TSP. This is mainly because the Trimer can generate large amounts of soot during combustion; high amounts of soot were detected instrumentally in the gas phase, which imply that the EVA/Trimer (30%) composite yields large amounts of smoke.

Hydrogen phosphate salt and pyrophosphate are the condensed phase decomposition products of AHP in the first and second steps, respectively [14]. These products can further promote the formation of a stable char residue in the condensed phase. Therefore, when AHP and Trimer are used together at an optimum ratio, the flame-retardant-loaded EVA sample had the lowest SPR, Av-SEA, PSPR, and TSP. However, the average CO yield (Av-COY) and the average CO_2 yield (Av-CO_2Y) of flame-retardant PVC are still higher than those of neat EVA.

The average effective heat of combustion (Av-EHC) for each composite is listed in Table 2. An increased EHC indicates a condensed phase effect in the flame retardant [26], and therefore EVA/Trimer (30%) exhibited the most significant condensed phase effect with the highest Av-EHC value of 76.89 MJ kg^{-1}; AHP has more obvious gas phase flame-retardant effect.

Thermogravimetric analysis (TG)

Figures 5 and 6 show the TG and DTG analysis curves, respectively, while Table 3 includes the corresponding details for EVA, EVA/AHP(30%), EVA/Trimer(30%), EVA/AHP/Trimer(7.5%), and EVA/AHP/Trimer(20%) under N_2, where the AHP/Trimer mass ratio was either 3:1 or 1:2.

The thermal degradation of EVA takes place in two steps. In the first step, vinyl acetate is degraded and the temperature at the maximum mass loss rate (T_{max1}) is

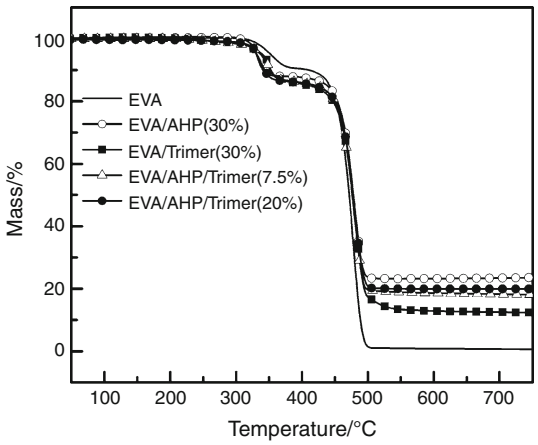

Fig. 5 TG curves of the EVA samples in N_2

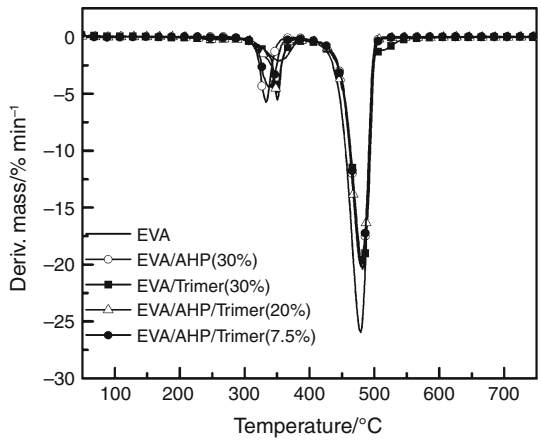

Fig. 6 DTG curves of the EVA samples in N_2

approximately 353 °C; in the second step, the polyene structure fractures and the temperature at the maximum mass loss rate (T_{max2}) is approximately 480 °C [25]. The main degradation products in the gas phase include CO, CO_2, H_2O, and ketones.

The decomposition process of AHP follows two stages; PH_3 and H_2O are the main gas phase products in the first and second steps of AHP decomposition, respectively. Hydrogen phosphate salt and pyrophosphate are the main condensed phase products, which can effectively promote the degradation of EVA in the first stage and enhance the stability of the polyene structure [14]. Although the decomposition temperature of Trimer is higher than that of EVA [14], the initial decomposition temperatures (defined as the temperature at which 5% of the initial mass has been lost, $T_{-5\ \%}$) of all the flame-retardant samples were lower than that of EVA. At the same time, the maximum mass loss rate in the first stage (R_{max1}) was increased significantly, while the maximum mass loss rate in the second stage (R_{max2}) reduced. These phenomena indicate an intumescent flame-retardant behavior; the addition of flame retardants catalyzes EVA decomposition in the first stage and generates a more stable char residue in the second stage. The char residue can effectively isolate heat and oxygen, and thus effectively promotes the flame retardancy and smoke suppression of EVA samples. These results are consistent with the cone test results.

SEM analysis of the char residue

The surface morphology of the char residue after the LOI test was investigated using SEM; the images are shown in Fig. 7. The morphology of the char layer formed by EVA containing AHP or Trimer in air is considerably different from that of the char layer formed by EVA containing AHP and Trimer after the LOI test. The char of the EVA samples containing AHP or Trimer has a porous structure. When AHP was combined with Trimer at the optimum proportions, the samples generated denser and stronger char residues; the char layer was generated rapidly after ignition, which was then intumesced by the emission of gaseous products that consequently formed an inside-to-outside air flow because of pressurization. Eventually, the flame was extinguished immediately after the igniter was removed, and thus, the dripping resistance and cone results were improved by the AHP and Trimer synergetic system.

Table 3 TG and DTG results of the flame-retardant EVA samples

samples	$T_{-5\%}$/°C	T_{max1}/°C	R_{max1}/% min^{-1}	T_{max2}/°C	R_{max2}/% min^{-1}	Residue at 750 °C/%
1	351.64	353.33	2.01	478.40	25.93	0.63
2	330.68	332.49	5.60	481.20	19.26	23.56
5	339.30	350.53	5.51	482.76	20.53	12.29
7	331.59	338.09	4.32	479.95	19.73	19.93
10	337.23	349.29	5.12	479.96	20.13	18.09

$T_{-5\ \%}$, the initial decomposition temperature; R_{max}, the maximum mass loss rate; T_{max}, the temperature at the maximum mass loss rate

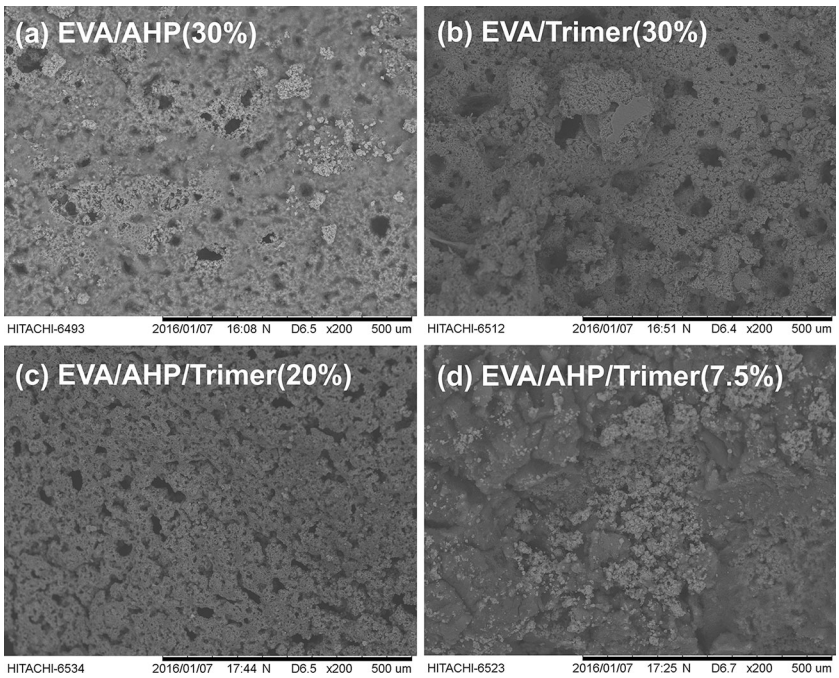

Fig. 7 SEM images of the char residues: **a** EVA/AHP (30%); **b** EVA/Trimer (30%); **c** EVA/AHP/Trimer (20%); **d** EVA/AHP/Trimer (7.5%)

Conclusions

The combustion properties of flame-retardant EVA were evaluated by LOI, UL-94 tests, and CCT. When AHP and Trimer were loaded together in EVA at a mass ratio of 3:1 and a total loading of 30 wt%, the LOI value and UL-94 rating were 24.4% and V-0, respectively. When exposed to a radiation of 50 kW m^{-2}, the PHRR and Av-HRR of EVA/AHP/Trimer (7.5%) were reduced by 67 and 28%, respectively, as compared to neat EVA. Additionally, Trimer alone can increase the quantity of smoke from the EVA samples; all of the SPR, PSPR, TSP, and Av-SEA exhibit different degrees of increase. On the contrary, the SPR, PSPR, TSP, and Av-SEA of EVA/AHP/Trimer (7.5%) are reduced. These results imply that considerable reductions in heat release and smoke emission can be achieved by combining AHP and Trimer. The TG and SEM analysis of the char residue results showed that the AHP and Trimer combination catalyzes EVA decomposition and generates a more stable char residue in the condensed phase, which can obviously improve the flame retardancy, smoke suppression, and dripping resistance of EVA.

Acknowledgements The work was financially supported by the Natural Science Foundation of China (Grant Nos. 21306035 and 21276059) and the Key Basic Research Project of Hebei Province (Grant No. 16961402D).

REFERENCES

1. Zhang F, Sun WY, Wang Y, Liu BS. Influence of the pentaerythritol phosphate melamine salt content on the combustion and thermal decomposition process of intumescent flame-retardant ethylene-vinyl acetate copolymer composites. J Appl Polym Sci. 2015;132(26):42148.
2. Lu K, Ye LJ, Liang QS, Li YJ. Selectively located aluminum hydroxide in rubber phase in a TPV: towards to a halogen-free flame retardant thermoplastic elastomer with ultrahigh flexibility. Polym Compos. 2015;36(7):1258–65.
3. Huang HH, Tian M, Liu L, Liang WL, Zhang LQ. Effect of particle size on flame retardancy of $Mg(OH)_2$-filled ethylene vinyl acetate copolymer composites. J Appl Polym Sci. 2006;100(6):4461–9.
4. Lv J, Qiu LZ, Qu BJ. Controlled synthesis of magnesium hydroxide nanoparticles with different morphological structures and related properties in flame retardant ethylene-vinyl acetate blends. Nanotechnology. 2004;15(11):1576–81.
5. Fu MZ, Qu BJ. Synergistic flame retardant mechanism of fumed silica in ethylene-vinyl acetate/magnesium hydroxide blends. Polym Degrad Stab. 2004;85(1):633–9.
6. Huang NH, Chen ZJ, Yi CH, Wang JQ. Synergistic flame retardant effects between sepiolite and magnesium hydroxide in ethylene–vinyl acetate (EVA) matrix. Express Polym Lett. 2010;4(4):227–33.
7. Ahamad A, Patil CB, Mahulikar PP, Hundiwale DG, Gite VV. Studies on the flame retardant, mechanical and thermal properties of ternary magnesium hydroxide/clay/EVA nanocomposites. J Elastom Plast. 2012;44(3):251–61.
8. Laoutid F, Lorgouilloux M, Lesueur D, Bonnaud L, Dubois P. Calcium-based hydrated minerals: promising halogen-free flame retardant and fire resistant additives for polyethylene and ethylene vinyl acetate copolymers. Polym Degrad Stab. 2013;98(9):1617–25.

9. Li L, Qian Y, Jiao CM. Synergistic flame retardant effects of ammonium polyphosphate in ethylene-vinyl acetate/layered double hydroxides composites. Polym Eng Sci. 2014;54(4):766–76.
10. Wang DY, Cai XX, Qu MH, Liu Y, Wang JS, Wang YZ. Preparation and flammability of a novel intumescent flame-retardant poly(ethylene-co-vinyl acetate) system. Polym Degrad Stab. 2008;93(12):2186–92.
11. Alongi J, Poskovic M, Frache A, Trotta F. Novel flame retardants containing cyclodextrin nanosponges and phosphorus compounds to enhance EVA combustion properties. Polym Degrad Stab. 2010;95(10):2093–100.
12. Wang XS, Pang HC, Chen WD, Lin Y, Ning GL. Nanoengineering core/shell structured brucite@polyphosphate@amine hybrid system for enhanced flame retardant properties. Polym Degrad Stab. 2013;98(12):2609–16.
13. Liu Y, Fang ZP. Combination of montmorillonite and a Schiff-base polyphosphate ester to improve the flame retardancy of ethylene-vinyl acetate copolymer. J Polym Eng. 2015;35(5):443–9.
14. Qu HQ, Liu X, Xu JZ, Ma HY, Jiao YH, Xie JX. Investigation on thermal degradation of poly(1,4-butylene terephthalate) filled with aluminum hypophosphite and Trimer by thermogravimetric analysis–Fourier transform infrared spectroscopy and thermogravimetric analysis–mass spectrometry. Ind Eng Chem Res. 2014;53(20):8476–83.
15. Liu X, Wang JY, Yang XM, Wang YL, Hao JW. Application of TG/FTIR TG/MS and cone calorimetry to understand flame retardancy and catalytic charring mechanism of boron phosphate in flame-retardant PUR–PIR foams. J Therm Anal Calorim. 2017;130(3):1817–27.
16. Yang W, Hong NN, Song L, Hu Y. Studies on mechanical properties, thermal degradation, and combustion behaviors of poly(1,4-butylene terephthalate)/glass fiber/cerium hypophosphite composites. Ind Eng Chem Res. 2012;51(24):8253–61.
17. Zhao B, Hu Z, Chen L, Liu Y. A phosphorus-containing inorganic compound as an effective flame retardant for glass-fiber-reinforced polyamide 6. J Appl Polym Sci. 2011;119(4):2379–85.
18. Yang W, Tang G, Song L, Hu Y. Effect of rare earth hypophosphite and melamine cyanurate on fire performance of glass-fiber reinforced poly(1,4-butylene terephthalate) composites. Thermochim Acta. 2011;526(1–2):185–91.
19. Yang W, Yuen RKK, Hu Y, Lu HD. Development and characterization of fire retarded glass-fiber reinforced poly(1,4-butylene terephthalate) composites based on a novel flame retardant system. Ind Eng Chem Res. 2011;50(21):11975–81.
20. Tang G, Wang X, Xing WY, Zhang P. Thermal degradation and flame retardance of biobased polylactide composites based on aluminum hypophosphite. Ind Eng Chem Res. 2012;51(37):12009–16.
21. Jiang W, Hao J, Han Z. Study on the thermal degradation of mixtures of ammonium polyphosphate and a novel caged bicyclic phosphate and their flame retardant effect in polypropylene. Polym Degrad Stab. 2012;97(4):632–7.
22. Zhuo JL, Xie LB, Liu GD, Chen XL, Wang YG. The synergistic effect of hollow glass microsphere in intumescent flame-retardant epoxy resin. J Therm Anal Calorim. 2017;129(1):357–66.
23. Chen XL, Li M, Zhuo JL, Ma CY. Influence of Fe_2O_3 on smoke suppression and thermal degradation properties in intumescent flame-retardant silicone rubber. J Therm Anal Calorim. 2016;123(1):439–48.
24. Pike RD, Starnes WH, Jeng JP, Bryant WS, Kourtesis P, Adams CW. Low-valent metals as reductive cross-linking agents: a new strategy for smoke suppression of poly(vinylchloride). Macromolecules. 1997;30(22):6957–65.
25. Zhang J, Ji KJ, Xia YZ. Polymer combustion and flame retardant technology. Beijing: Chemical Industry Press; 2005. p. 130–2.
26. Feng J, Hao JW, Du JX, Yang RJ. Using TGA/FTIR TGA/MS and cone calorimetry to understand thermal degradation and flame retardancy mechanism of polycarbonate filled with solid bisphenol A bis(diphenyl phosphate) and montmorillonite. Polym Degrad Stab. 2012;97(4):605–14.